



Indomethacin-containing interpolyelectrolyte complexes based on Eudragit® E PO/S 100 copolymers as a novel drug delivery system

Article

Accepted Version

Creative Commons: Attribution-Noncommercial-No Derivative Works 4.0

Moustafine, R. I., Sitenkov, A. Y., Bukhovets, A. V., Nasibullin, S. F., Appeltans, B., Kabanova, T. V., Khutoryanskiy, V. V. and Guy, V. d. M. (2017) Indomethacin-containing interpolyelectrolyte complexes based on Eudragit® E PO/S 100 copolymers as a novel drug delivery system. *International Journal of Pharmaceutics*, 524 (1-2). pp. 121-133. ISSN 0378-5173 doi: <https://doi.org/10.1016/j.ijpharm.2017.03.053>
Available at <http://centaur.reading.ac.uk/69988/>

It is advisable to refer to the publisher's version if you intend to cite from the work.

Published version at: <http://www.sciencedirect.com/science/article/pii/S0378517317302296>

To link to this article DOI: <http://dx.doi.org/10.1016/j.ijpharm.2017.03.053>

Publisher: Elsevier

All outputs in CentAUR are protected by Intellectual Property Rights law, including copyright law. Copyright and IPR is retained by the creators or other copyright holders. Terms and conditions for use of this material are defined in

the [End User Agreement](#).

www.reading.ac.uk/centaur

CentAUR

Central Archive at the University of Reading

Reading's research outputs online

1 Indomethacin-containing 2 interpolyelectrolyte complexes based on 3 Eudragit® E PO/S 100 copolymers as a 4 novel drug delivery system

5 Rouslan I. Moustafine^{1*}, Alexander Y. Sitenkov¹, Alexandra V. Bukhovets¹, Shamil F. Nasibullin¹,
6 Bernard Appeltans², Tatiana V. Kabanova¹, Vitaliy V. Khutoryanskiy³, Guy Van den Mooter²

7
8 ¹Department of Pharmaceutical, Analytical and Toxicological Chemistry, Kazan State Medical University,
9 Butlerov Street 49, 420012 Kazan, Russian Federation

10 ²Drug Delivery and Disposition, University of Leuven (KU Leuven), Leuven, Belgium

11 ³Reading School of Pharmacy, University of Reading, Whiteknights, Reading RG66AD, Berkshire, United
12 Kingdom

13 *Corresponding author: rouslan.moustafine@gmail.com

14 Abstract

15 *Potential applications of a novel system composed of two oppositely-charged (meth)acrylate*
16 *copolymers, Eudragit® EPO (EPO) and Eudragit® S100 (S100), loaded with indomethacin (IND) in*
17 *oral drug delivery were evaluated. The particles based on drug-interpolyelectrolyte complexes*
18 *(DIPEC), (EPO-IND)/S100, were prepared by mixing aqueous solutions of both copolymers at fixed*
19 *pH. Particles of drug-polyelectrolyte complex (DPC), (EPO-IND) have a positive zeta potential,*
20 *pointing to the surface location of free EPO chains and IND bound to EPO sequences. The*
21 *formation and composition of both DPC and DIPEC were established by gravimetry, UV-*
22 *spectrophotometry, capillary viscosity and elemental analysis. The structure and solid state*
23 *properties of the formulated DIPEC were investigated using FTIR/NIR, Raman spectroscopy, XRPD*
24 *and modulated DSC. DIPEC is a chemically homogenous material, characterized by a single T_g.*
25 *DIPEC have an IR absorption band at 1560 cm⁻¹, which can be assigned to the stretching vibration of*
26 *the carboxylate groups (S100, IND) that form ionic bonds with the dimethylamino groups of EPO.*
27 *XRPD, NIR and Raman-shifts confirm that during the preparation of this formulation, IND is*
28 *converted into its amorphous form. The release of IND from DPC EPO/IND (3:1) and DIPEC*
29 *EPO/L100/IND (4.5:1:1) is sustained and is completed within 7 hours under GIT mimicking*
30 *conditions. However, S100 within DIPEC makes the release process slower making this system*
31 *suitable for colon-specific delivery. Finally, DPC and DIPEC with indomethacin were used to*
32 *prepare tablets, which can be potentially used as oral dosage forms for their slower*
33 *indomethacin release in case of DIPEC which could be suitable for sustained delivery.*

34 Keywords

35 Drug-interpolyelectrolyte complexes; drug-polyelectrolyte complexes; Eudragit® EPO; Eudragit® S100;
36 Indomethacin; Oral drug delivery.

39 **1. Introduction**

40 The advantages of interpolymer complexes as polymeric carriers in oral controlled drug release have been
41 reported elsewhere (Kemenova et al., 1991; Hartig et al., 2007; Khutoryanskiy, 2007; Lankalapalli and
42 Kolapalli, 2009; Pillay et al., 2013, Bourganis et al., 2017). In the last years, our research group has developed
43 polycomplex matrices based on interpolyelectrolyte complexes (IPECs) using different oppositely-charged
44 Eudragit® copolymer combinations as new oral delivery systems able to deliver the drugs into site-specific
45 gastrointestinal tract (GIT) regions (Mustafin and Kabanova, 2004, 2005; Moustafine et al., 2005, 2006, 2011,
46 2013; Moustafine and Bobyleva, 2006; Mustafin et al., 2010a, 2010b, 2011). Moreover, the advantages of
47 Eudragit® copolymer combinations for controlled drug delivery purposes have been reported elsewhere
48 (Siepmann et al., 2008; Obeidat et al., 2008; Sauer and McGinity, 2009; Alhnan and Basit, 2011; Bani-Jaber,
49 et al., 2011; Wulff and Leopold, 2014, 2016).

50 The comprehensive analysis of the effects of intermacromolecular interactions between chemically
51 complementary Eudragits® on the drug release from oral drug delivery systems (DDS) was examined in
52 recently published reviews (Gallardo et al., 2008; Mustafin, 2011, Moustafine, 2014; De Robertis et al., 2015).
53 However, further studies are needed to address more complex systems involving oppositely-charged
54 Eudragits® forming IPECs in the presence of ionic drugs. Only a few papers reported the possibility of using
55 drug-interpolyelectrolyte complexes (DIPEC) as three-component systems for development of drug delivery
56 dosage forms (Palena et al., 2012, 2015; Bigucci et al., 2015).

57 Recently, a novel self-organized nanoparticulate carrier, based on drug – IPEC Eudragit® E100/L100
58 combination was successfully prepared using a simple aqueous dispersion method (Palena et al., 2012). In
59 this study, the authors have reported that freeze-dried complexes were easily redispersed in water and DIPEC
60 dispersions behaved as zwitterionic macromolecular systems that may change zeta potential values from
61 negative to positive by changing the polymer composition. The authors have used atenolol, propranolol and
62 metoclopramide as model drugs, which could be formulated using these nanoparticulate systems. Recently
63 four additional anti-inflammatory drugs (salicylic acid, benzoic acid, ketoprofen and naproxen) were also
64 studied (Palena et al., 2015). The DIPECs exhibited interesting properties useful for the design of
65 nanoparticulate DDS for oral and topical administration.

66 Furthermore, a similar principle was successfully used in a chitosan/carboxymethylcellulose polyelectrolyte
67 system via electrostatic interaction between the amino groups of chitosan and chlorhexidine (cationic drug)
68 with the carboxyl groups of sodium carboxymethylcellulose, used for the preparation of vaginal inserts
69 (Bigucci et al., 2015).

70 The objective of this study was the preparation and physicochemical characterization of drug-
71 interpolyelectrolyte complexes (DIPEC) as micro-sized particles formed between indomethacin and Eudragit®
72 S100 with oppositely-charged Eudragit® EPO. These microparticles were found to be highly promising
73 materials for designing pH-controlled systems for oral delivery to target the colon. Colon-specific drug

74 delivery systems are of interest for the therapy of different local conditions such as ulcerative colitis, Crohn's
75 disease, irritable bowel syndrome, chronic pancreatitis, and colonic cancer (Basit, 2005; Gazzaniga, 2006; Van
76 den Mooter, 2006, Maroni et al., 2013; Amidon et al., 2015; Hua et al., 2015). Different approaches have
77 been traditionally used in drug delivery for colon targeting, including the use of prodrugs, pH-responsive
78 matrix systems, timed-release formulations, bioadhesive materials, microparticulate vehicles and enteric
79 coatings (Amidon et al., 2015). Our approach involves the use of conventional enteric coating polymer
80 Eudragit® S100 that already provides gastric resistance properties; additionally, in our work we utilised the
81 ability of this anionic polymer to form interpolyelectrolyte complexes with cationic Eudragit® EPO. The
82 functionality of both polymers provided an opportunity of forming polycomplex particles with indomethacin
83 and formulate tablets with sustained drug release.

84 **2. Materials and methods**

85 **2.1 Materials**

86 Eudragit® E PO – a terpolymer of *N,N*-dimethylaminoethyl methacrylate (DMAEMA) with methylmethacrylate
87 (MMA) and butylmethacrylate (BuMA), (PDMAEMA-*co*-MMA-*co*-BMA) (mole ratio 2:1:1, MW 150 kDa) was
88 used in this study as a cationic copolymer. Eudragit® S 100 (a copolymer of methacrylic acid (MAA) with
89 methylmethacrylate (MMA), P(MAA-*co*-MMA) (mole ratio 2:1, MW 135 kDa)) was used as a polyanion.
90 Different types of Eudragit® (EPO, S100) were generously donated by Evonik Röhm GmbH (Darmstadt,
91 Germany). The copolymers were used after vacuum drying at 40°C for 2 days. The solutions at different pH
92 values, simulating the gastrointestinal conditions, were prepared for release tests by using hydrochloric acid,
93 sodium phosphate tribasic dodecahydrate, potassium dihydrogen phosphate, and sodium hydroxide (Sigma-
94 Aldrich, Bornem, Belgium). IND was used as a model anionic drug and was purchased from Sigma-Aldrich
95 (Bornem, Belgium).

96 **2.2. Methods**

97 **2.2.1 Preparation of solid DPCs and DIPECs with different macromolecular composition**

98 The optimal conditions for the interaction between chemically complementary grades of a polycation
99 (Eudragit® EPO) and a polyanion copolymer (Eudragit® S100) in the presence of ionized IND molecules were
100 studied in aqueous salt media. EPO solutions were prepared by dissolving the copolymer in 1 M CH₃COOH.
101 This solution was diluted with demineralized water to the desired volume and titrated with 1 M NaOH to the
102 required pH 6.5. S100 and IND solutions were prepared by dissolving the copolymer and the drug in 1 M
103 NaOH. This solution was diluted with demineralized water to the desired volume and titrated with 1 M
104 CH₃COOH to the required pH 7.2. The EPO solutions were slowly poured into S100/IND solutions, and the

105 mixture was stirred at 1000 r.p.m. for 2 days using a magnetic stirrer RET control visc-white (IKA®, Staufen,
106 Germany). The solutions of copolymers and IND were mixed in different molar ratios. The yields of precipitate
107 formed were first determined gravimetrically after centrifugation for 1 h at 5000 rpm at 5 °C in a SL16R
108 laboratory centrifuge (Thermo Scientific, U.S.A.). The specific viscosity of the supernatant solution was
109 determined using an Ubbelohde viscometer (Schott®, Germany) at 25.0±0.1 °C. The quantity of the non-
110 bonded IND present in the supernatant solutions and the encapsulation efficiency (EE) were investigated UV-
111 spectrophotometrically at 266 nm (Evolution 220, Thermo Scientific, U.S.A.). For gravimetric determination,
112 the sediment was dried under vacuum (vacuum oven VD 23, Binder, Germany) for 2 days at 40 °C until
113 constant weight.

114 The optimal composition was prepared in a laboratory reactor system LR 1000 control equipped with pH-
115 /temperature controlling units under continuous and simultaneous agitation at 10,000 r.p.m. using T25-
116 digital Ultra-Turrax® homogenizer (IKA®, Staufen, Germany). The feeding rate was approximately 2 mL/min.
117 After isolation of the precipitates of DPC and DIPEC particles from solutions, they were washed with ultrapure
118 water (Smart2Pure UV/UF, Thermo Scientific, U.S.A.), frozen at -18 °C (Labconco® Shell Freezer, MO, U.S.A.)
119 and subsequently freeze-dried for 2 days (Labconco® Freeze Dry System, FreeZone 1 L, MO, U.S.A.). The solid
120 samples were stored in tightly-sealed containers at room temperature.

121 **2.2.2 Elemental analysis**

122 The composition of freeze-dried DPC (EPO/IND) and DIPEC (EPO/L100/IND) samples and physical mixtures
123 were investigated by elemental analysis using a Thermo Flash 2000 CHNS/O elemental analyzer (Thermo
124 Scientific, UK). Physical mixtures were obtained by mixing copolymer powders and IND at EPO:S100:IND
125 molar ratio of 4.5:1:1.

126 **2.2.3 Fourier Transform Infrared Spectroscopy (ATR-FTIR)**

127 ATR-FTIR-spectra were recorded using a Nicolet iS5 FTIR-spectrometer (Thermo Scientific, U.S.A.) equipped
128 with a DTGS detector. The untreated freeze-dried samples of solid DPC (EPO/IND), DIPEC (EPO/S100/IND)
129 and physical mixtures were directly mounted over the iD5 smart single bounce ZnSe ATR crystal. The spectra
130 were analyzed using OMNIC spectra software.

131 **2.2.4 Near-infrared (NIR) spectroscopy**

132 NIR-spectroscopy of freeze-dried samples of solid DPC (EPO/IND), DIPEC (EPO/S100/IND) and physical
133 mixtures was performed using a Nicolet iS10 XT NIR/FTIR-spectrometer (Thermo Scientific, U.S.A.) equipped
134 with Smart DRA diffusion reflection accessory. The spectra were analyzed using OMNIC spectra software.

135 **2.2.5 Particle characterization**

136 Particle sizes and zeta potential (ZP) of DIPEC particles in aqueous dispersion were evaluated using a Zetasizer
137 Nano ZL (Malvern Instruments Ltd., Worcestershire, UK). Solid state particles characterization of freeze-dried

138 DIPEC (EPO/S100/IND) samples was performed on the Morphologi G3SE-ID automated system (Malvern
139 Instruments Ltd., Worcestershire, UK) equipped with fiber-optics Raman-spectrometry (RamanRxn1™
140 Analyzer, Kaiser Optical Systems, INC., Germany).

141 **2.2.6 Thermal analysis**

142 Modulated DSC (MDSC) measurements were carried out using a Discovery DSC™ (TA Instruments, New Castle,
143 DE, U.S.A.), equipped with a refrigerated cooling system (RCS90). TRIOS™ software (version 3.1.5.3696) was
144 used to analyze the obtained data (TA Instruments, New Castle, DE, U.S.A.). Tzero aluminum pans (TA
145 Instruments, New Castle, DE, U.S.A.) were used in all calorimetric studies. The empty pan was used as a
146 reference and the mass of the reference pan and of the sample pans were taken into account. Dry nitrogen
147 at a flow rate of 50 mL/min was used as a purge gas through the DSC cell. Indium and *n*-octadecane standards
148 were used to calibrate the DSC temperature scale; enthalpic response was calibrated with indium. The
149 modulation parameters used were: 2 °C/min heating rate, 40 s period and 1 °C amplitude. Calibration of heat
150 capacity was done using sapphire. Samples were analyzed from 0 to 250 °C. Glass transitions were analyzed
151 in the reversing heat flow signals.

152 Thermogravimetric analysis (TGA) was performed using Discovery TGA™ (TA Instruments, New Castle, DE,
153 U.S.A.). Samples (10-15 mg) were placed on an aluminum pan and heated from 25 to 190 °C at 10 °C/min.
154 Resulting weight-temperature diagrams were analyzed using TRIOS™ software (version 3.1.5.3696) to
155 calculate the weight loss between 25 and 170 °C.

156 **2.2.7 X-ray powder diffraction**

157 X-ray powder diffraction (XRPD) was performed on the freeze-dried samples of solid DIPEC (EPO/S100/IND)
158 and physical mixtures. An automated XPERT-PRO diffractometer system (PANalytical, Almelo, the
159 Netherlands) was used in reflection mode. All samples were measured without crushing or any other sample
160 processing. A copper tube with the generator set at 45 kV and 40 mA was used. Using a transmission spinner,
161 it was possible to improve the counting statistics by spinning the sample using a rotation time of 4.0 s. In the
162 incident beam path, 0.04 rad soller slit and a programmable divergence slit of 10 mm were applied. In the
163 diffracted beam path, 0.04 rad soller slit and programmable anti-scatter slit were installed. The detector used
164 for data collection was an X'Celerator RTMS detector, with an active length of 2.122°. The data were collected
165 in continuous scan mode with a scan range of 4.0040-40.001° and a step size of 0.0167°. The counting time
166 was 499.745 s. X'Pert Data Collector version 2.2a (PANalytical, Almelo, the Netherlands) was used for data
167 collection and X'Pert Data Viewer version 1.2.a (PANalytical, Almelo, the Netherlands) was used for data
168 visualization and treatment.

169 **2.2.8 Release of indomethacin from the particles under GIT mimicking conditions**

170 The release of IND from the DDS was performed under sink conditions at 37.0±0.1 °C using the USP II
171 Apparatus (the off-line dissolution tester DT 828 with an auto sampler ASS-8, a fraction collector FRL 824 and

172 a peristaltic pump ICP-8 (Erweka, Heusenstamm, Germany)). The paddles rotation speed was 100 rpm. The
173 release was investigated for 7 hours under GIT mimicking conditions, where the pH of the release medium
174 was gradually increased: 1 hour in 0.1 M hydrochloric acid (pH=1.2), 2 hours in phosphate buffer solution
175 (pH=5.8), 2 hours in phosphate buffer solution (pH=6.8), and finally in phosphate buffer solution (pH=7.4)
176 until the end of the experiment (Lorenzo-Lamoza et al., 1998).

177 A weighted amount of the DDS (50 mg; estimated to contain approx. 10 mg IND) was suspended in 400 mL
178 of 0.1 M hydrochloric acid, then 400 mL of 0.02 M dibasic potassium phosphate trihydrate were added in the
179 release media after 1 hour. Then the pH of the resulting solution was adjusted to the desired pH (5.8, 6.8,
180 and 7.4) with sodium hydroxide. Final volume was kept at 850 mL. pH control was carried out in each vessel
181 with a portable pH meter Orion Star A 325 (Thermo Scientific, U.S.A.) using the Orion™ ROSS Ultra™ low
182 maintenance pH/ATC Triode™ (Thermo Scientific, U.S.A.). At fixed time intervals, 5 mL of the solution was
183 withdrawn, filtered through a syringe filter with a pore diameter of 0.45 microns (Supelco Iso-Disc Filters N-
184 25-4 Nylon 25 mm) and the amount of IND released was analyzed by UV spectrophotometry (Lambda 25,
185 Perkin Elmer, U.S.A.). IND presence in all performed tests was detected by recording the full absorption
186 spectra in the wavelength range from 200 to 400 nm and identifying the peak height closest to 330 nm to
187 avoid incorrect measurements due to the shift in λ_{max} : a spectrum fitting procedure was adopted instead of
188 the simple reading of the absorbance at given wavelength, being much more effective to eliminate any
189 possible interferences due to copolymers (Dalmoro et al., 2016) or DPC and DIPEC formation. An equal
190 volume of the same dissolution medium was replaced to maintain a constant volume. The experiments were
191 performed in triplicate.

192 **2.2.9 DIPEC particles characterization under GIT mimicking conditions**

193 Measurements of the size and zeta potential of the DIPEC particles under conditions, mimicking the release
194 process was also performed using the Zetasizer Nano ZS equipped with multi-purpose titrator MPT-2 and
195 degasser accessories (Malvern Instruments Ltd., Worcestershire, UK). Samples of DIPEC particles were
196 redispersed in 0.1 M hydrochloric acid (pH 1.2). Then 0.1 M sodium hydroxide solution was gradually added
197 to the dispersion of DPC by using an automatic titrator, until a pH of 7.4 was reached. During the titration,
198 the zeta potential and size of the polymer-drug complex were measured between pH 1.2-7.4.

199 All the experimental determinations were performed in triplicate; the results were expressed as average
200 values with standard deviation (SD).

201 **2.2.10 Tablet preparation and indomethacin release under GIT mimicking conditions**

202 With the aim to study the IND release from tablets as possible oral dosage systems, the produced loaded
203 particles were used to prepare tablets by the following procedures. Tablets with IND loaded particles (DPC
204 and DIPEC) were prepared by compressing about 500 mg of lyophilized particles (estimated to contain
205 approx. 100 mg IND) in a hydraulic press for FTIR (Perkin Elmer, U.S.A.), equipped with flat-faced punches

206 with 13 mm diameter (by a Pike Technologies, U.S.A.) with a compression pressure of 2.45 MPa. The same
207 procedure was applied to 500 mg of physical mixtures and IND powder (the compositions were similar to
208 DPC and DIPEC ratios, respectively). The two kinds of produced tablets were then subjected to in vitro drug
209 release studies applying the method used for IND release from uncompressed particles, previously described.
210 All the experimental determinations were performed in triplicate; the results were expressed as average
211 values \pm standard deviation (SD).

212 **3. Results and discussion**

213 **3.1 Preparation and characterization of DPC and DIPEC particles**

214 EPO is soluble in acidic solutions up to pH 7.0 (Mustafin et al., 2011), due to hydration of protonated
215 dimethylamino groups. On the other hand, S100 is soluble above pH 7.0 due to hydration of ionized carboxyl
216 groups. IND is a non-steroidal anti-inflammatory drug containing an acidic function with a $pK_a = 4.5$ (Priemel
217 et al., 2013a, 2013b; De Filippis et al., 1991). The possibility of interaction between these two polyelectrolytes
218 and IND was investigated between pH 6.8 and 7.2, where both copolymers and the drug are soluble and
219 partially ionized.

220 EPO-IND polycomplex formation was first investigated using gravimetric analysis of precipitates and UV-
221 spectrophotometry analysis of supernatant solutions, prepared at different molar ratios at pH 6.5. At this pH,
222 the degree of ionization and charge density of EPO is very small. In contrast, the reaction capability of the drug
223 is high. Fig. 1a shows that the maximum of the precipitate yield corresponds to the maximum of bound IND.
224 The maximum of EPO/IND polycomplex yield was found at the unit molar ratio of 3:1. The observed binding
225 molar ratio corresponds to the stoichiometry of the obtained DPC EPO/IND, estimated also by elemental
226 analysis of the dry DPC precipitates.

227 The next step was to determine the optimal composition in DIPEC (EPO/S100/IND) mixtures. Fig. 1b shows
228 the results of precipitate and supernatant analysis, which confirm that the stoichiometric composition of
229 precipitated DIPEC (EPO/S100/IND) corresponds to the molar ratio of 4.5:1:1.

230 **3.1.2 Compositional study**

231 Fig. 2 shows the apparent viscosity of the supernatant in EPO/S100/IND mixtures. The decrease in viscosity
232 observed in EPO/S100/IND mixtures showed that the insoluble DIPEC was formed in the investigated medium
233 and was removed by centrifugation (Cilurzo et al., 2000, Moustafine et al., 2005). A minimum in the curve is
234 observed when the mixture of EPO/S100/IND was 4.5:1:1. Thus, the DIPEC is enriched with the less ionized
235 component (charge density on EPO chains > 0). On the other hand, an incorporation of the anionic
236 components (S100 and IND) decreases due to the progressive increase in the fraction of ionized carboxylic
237 acids. This also increases the drug reactivity. In order to confirm the proportion of each component in the

238 solid DIPEC, elemental analysis of the dry precipitates was performed. The results are summarized in Table 1
239 and clearly indicate that the molar ratio between EPO, S100 and IND in the triple polycomplex is 4.5:1:1.

240 **3.1.3 Morphological and dimensional analysis**

241 The particle size of freshly prepared DIPEC particles was determined by photon correlation spectroscopy.
242 DIPEC particles showed a mean diameter (MD) of 497 ± 51 nm with a positive value of zeta potential (+17.4
243 mV), pointing to the surface location of free EPO chains and IND bound to EPO sequences.

244 Additionally, particle size distribution and morphological analysis of the DIPEC samples was estimated. Three
245 main groups of particle size were observed (*Fig. S1a, Supporting Information*): small (mean diameter (MD) \leq
246 300 nm; 98.06%), medium ($300 \text{ nm} \leq \text{MD} \leq 10 \text{ }\mu\text{m}$; 1.90%) and large ($\text{MD} \geq 10 \text{ }\mu\text{m}$; 0.04%). *Fig. S2b (Supporting*
247 *Information)* summarized the results of the morphological analysis, in the case of the “large” group, and
248 shows nearly spherical morphology (according to the circularity measurements) of the particles and a low
249 degree of aggregation. Similar morphology was found for the other two groups of particles (data not shown).
250 All of the evaluated particles have circularity values close to 1 indicating nearly perfect spheres. Moreover,
251 identification of the particles included from the “small” group (making up the majority of particles) by Raman-
252 spectrometry showed that these particles consist of DIPEC (94%) and do not contain free IND (*Fig. S2c,*
253 *Supporting Information*).

254 **3.1.4 Drug encapsulation**

255 Direct encapsulation of IND was achieved by preparing particles in the presence of EPO and S100 and
256 formation of IPEC between these oppositely-charged copolymers. The residual amount of IND at the end of
257 the particles preparation was evaluated by UV-spectrophotometry. The data showed that encapsulation
258 efficiency (EE) was 75.6% (Table 2). The high EE is most likely the consequence of strong interactions between
259 IND molecules and EPO which is simultaneously bound to the countercharged S100 sequences.

260 **3.2 Evaluation of the DIPEC structure**

261 **3.2.1 Mid-infrared spectroscopy**

262 FTIR spectra indicate that IND is present as the γ -form showing absorption peaks at 1714 and 1690 cm^{-1} (*Fig.*
263 *3a*) (Liu et al., 2010, 2012; Chokshi et al., 2005, 2008; Sarode et al., 2013a, 2013b). The FTIR spectra of the
264 physical mixture of IND and copolymers (EPO and S100) in the same as in DIPEC ratio, is virtually a superposition
265 of the spectra of all components (*Fig. 3b*). However, the DPC and DIPEC show a different absorption band at
266 1560 cm^{-1} , which is due to the stretching vibration of the carboxylate groups that form the ionic bonds with the
267 protonated dimethylamino groups of EPO (*Fig. 3c,d*). Although Liu et al. (2010) reported that ionic interactions
268 between ionized carboxylic groups of IND and oppositely charged dimethylamino groups of EPO in IND/EPO solid
269 dispersions result in a broad absorption band at 2479 cm^{-1} which corresponds to ionized amino groups, we did
270 not observe this in spite of similar levels of drug loading. This can be explained since the charge density of the

271 EPO macromolecules decreases smoothly at the pH of DIPEC preparation. Moreover, in this study, we have a
272 system with a significantly higher complexity since the amino groups of EPO can interact not only with IND but
273 simultaneously with S100. The existence of non-ionized dimethylamino groups (2770 and 2820 cm^{-1}) in DIPEC
274 indicates that in this structure, they are localized mainly in 'defects' together with ionized bound groups of EPO
275 which is largely dependent on the conditions of the DIPEC preparation. The ratio of non-ionized and ionized
276 dimethylamino groups depends on the charge density of EPO macromolecules that is relatively low at pH
277 6.8–7.2.

278 The peak of the carbonyl stretching vibration (belonging to the carboxyl group) of IND at 1714 cm^{-1} completely
279 overlapped with a strong band of carbonyl stretching vibration of EPO and S100 at 1730 cm^{-1} . Therefore, we
280 focused on the region of near-infrared spectroscopy in order to evaluate potential IND transformations (from
281 γ -form to α -form or to the amorphous form) (Tanabe et al., 2012; Heinz et al., 2007; Nielsen et al., 2012).

282 **3.2.2 Near-infrared spectroscopy**

283 Due to the complexity of DPC and DIPEC systems, the main differences between the crystalline and
284 amorphous forms were observed from 1650 nm to 1900 nm (Heinz et al., 2007). Indeed, a peak at 1860 nm
285 resulting from the vibrations of the carboxylic group observed in the spectra of γ -form IND was absent both
286 in physical mixtures, DIPEC and DPC (Fig. 4a). Therefore, in the ternary physical mixture and DIPEC, IND could
287 not exist in a γ -form. Moreover, the peak at 1666 nm in IND powder confirms the presence of amorphous
288 form too, which also appeared in DPC and DIPEC, but not in a physical mixture. In case of IND and physical
289 mixture a peak maximum at 1696 nm confirms the existence of γ -form IND, which is absent in DPC and DIPEC.
290 Interestingly, the appearance of a new peak at 1702 nm for DIPEC is also observed in NIR-spectra of the
291 individual copolymers – EPO and S100, but not in their physical mixture (Fig. 4b). NIR-spectroscopy thus
292 confirmed the presence of individual copolymers (EPO and S100) in the structure of DIPEC, due to the
293 appearance of the peaks at 1702 nm, and the amorphous form of IND (the peak at 1666 nm).

294 **3.2.3 Raman spectroscopy**

295 Raman-spectra were recorded to further characterize the solid-state of IND in DIPEC, and the possible
296 interactions between sequences of countercharged copolymers (EPO, S100) and anionic drug (IND). For
297 characterization of IND, the 1715–1100 cm^{-1} spectral range was used (*Figure S2a, Supporting Information*).
298 The vibrational mode occurring at 1699 cm^{-1} confirmed the existence of γ -form of IND (Heinz et al., 2007; Kao
299 et al., 2012; Hedoux et al., 2008), which is also present in a physical mixture. The spectrum of the physical
300 mixture can be regarded as the superposition of the spectra of IND, EPO and S100. However, in the DIPEC
301 particles, a new peak appeared at 1680 cm^{-1} , which corresponds to the amorphous form of IND (Heinz et al.,
302 2007; Kao et al., 2012). Both peaks are assigned to the benzoyl carbonyl stretching vibration (Hedoux et al.,
303 2008). Molecules of γ -form of IND are mostly organized in cyclic dimers linked by hydrogen bonds (Chokshi
304 et al., 2005; Hedoux et al., 2008). The absence of low frequency mode at 200 cm^{-1} (*Fig. S2a, Supporting*

305 *Information*) in the Raman spectrum of DIPEC (which is present in IND spectrum) is also a confirmation of the
306 formation of an amorphous phase since this peak corresponds to the phonon of γ -form with long-range
307 crystalline order (Hedoux et al., 2008).

308 Therefore, both methods (NIR- and Raman- spectroscopy) confirm the transformation of the γ - form of IND
309 into the amorphous form during the preparation of DIPEC particles. However, Raman spectroscopy was not
310 suitable for establishing inter-macromolecular interactions between the copolymers (*Fig. S2b, Supporting*
311 *Information*).

312 **3.2.4 Thermal and XRPD analysis**

313 In order to further support the observed appearance of the amorphous IND form established with FTIR-,
314 NIR- and Raman spectroscopy and to bring further evidence that the formation of DIPEC between EPO and
315 IND in the presence of S100 is the result of an electrostatic interaction between these copolymers and the
316 drug, MDSC experiments were performed.

317 The γ -form of IND shows an endothermic peak at 160.2 °C, corresponding to the melting point (T_m). The glass
318 transition temperature (T_g) of the amorphous form is located at ca. 46.0 °C which is in accordance with the
319 literature (Liu et al., 2010, 2012; Sarode et al., 2013a, 2013b). Eudragit® copolymers are amorphous
320 substances and have a characteristic T_g : EPO (52.1°C) and S100 (160.7 °C).

321 Physical mixtures made of EPO/S100/IND showed two T_g values, one at 50.8±1.1°C and a second one at
322 152.5±1.3°C related to EPO and S100. Transitions belonging to IND were not observed (data not shown).

323 Moreover, MDSC was used to confirm the structural differences between DIPEC and physical mixtures
324 identified by FTIR spectroscopy, as well as to evaluate the chemical homogeneity of the copolymer-drug
325 systems by the absence of microdomains of free copolymers and IND. The thermal characteristics of DIPEC
326 vary with their composition and are given in Table 3. The data recorded for DIPEC demonstrates the
327 amorphous nature of this system and copolymer miscibility since a single T_g (70.8 °C) was observed (Sipos et
328 al., 2008). Also, the DPC (IND/EPO) is a miscible amorphous system displaying a single T_g at 43.7 °C.

329 To ensure that IND did not degrade during the heating, the DIPEC was studied using thermogravimetric
330 analysis. No appreciable weight loss was observed after heating at 170 °C for 10 min in a nitrogen
331 environment (data not shown). Liu et al. also reported that no significant degradation was observed upon
332 heating to prepare solid dispersions of IND and EPO at 170 °C (Liu et al., 2012).

333 XRPD analysis (*Fig. S3, Supporting Information*) confirmed the MDSC data that IND is present in the
334 amorphous form in PDC and DIPEC.

335 **3.3 Pharmaceutical evaluation of DPC and DIPEC**

336 **3.3.1 Indomethacin loaded particles: release tests**

337 In a further set of experiments, we tested the potential of DPC to be used in drug delivery systems to control the
338 release of IND.

339 In vitro IND release experiments within 7 hours in GIT mimicking conditions for pure IND, DPC and DIPEC
340 showed the potential of DIPEC (EPO/L100/IND 4.5:1:1) to be used as a carrier, suitable for colon-specific drug
341 delivery (Fig. 5).

342 The results could be understood if we consider the structure of the formed DIPEC in depth. It is well known, that
343 there are two main classes of IPECs: stoichiometric IPECs, which include the polymers in equimolar ratio and
344 non-stoichiometric IPECs that have excessive amount of one of the polyelectrolytes. The last one is also called
345 soluble IPECs because of their solubility in water (Philipp et al., 1989; Tsuchida, 1994; Thünemann et al.,
346 2004; Kabanov, 2005; Pergushov et al., 2012). Moreover, in the structure of IPECs two types of chains can be
347 distinguished: the interacting chains, which belong to both interacting polymers; and the loops, which are
348 also called “defects” of non-interacting chains due to steric hindrances (Kabanov et al., 2005). According to
349 this, the process of DIPEC formation may be divided into three main steps: (1) drug-interpolyelectrolyte
350 complex formation by simultaneous interactions of EPO with oppositely-charged IND and S100; (2)
351 transformation to a thermodynamically stabilized system by migration of ionic bonds; (3) drug-
352 interpolyelectrolyte complex aggregation process and formation of microparticles. The first step is realized
353 through binding via electrostatic attraction forces. The second step involves the formation of new bonds
354 and/or the correction of the distortions of the polymer chains. The third step involves the aggregation of
355 polycomplex particles, possibly through hydrophobic interactions.

356 The structure “defects” formed during the preparation of DIPEC do not only contain non-ionized dimethylamino
357 groups of EPO and ether groups of both copolymers, as it could be in a stoichiometric IPEC structure, but also
358 ionized dimethylamino groups that interact with carboxylate groups of IND and S100. Moreover, due to the non-
359 stoichiometric structure of DIPEC, containing three-fold excess of EPO, additional sequences of EPO are able
360 to interact with oppositely-charged IND molecules and S100. As a result, the structure of IPEC is changed
361 because the ionic bonds are not fixed and they can migrate from one electrostatic site to another (Kabanov et
362 al., 2005). The only problem is that at a pH between 6.8 and 7.2, the charge density of EPO macromolecules is
363 low. This means that more sequences of EPO are needed to achieve optimal encapsulation efficiency of IND
364 molecules. Moreover, equimolecular amounts of S100 could bind a similar molar amount of EPO during
365 formation of microparticles. Thus, ionized dimethylamino groups are interacting with ionized carboxylic acid
366 groups of IND in the sequences included in the loops and can also form new interpolymer contacts with S100.

367 The carboxylic groups of S100 that are present in “defects” are ionized at pH 7.0 and consequently increase the
368 degree of ionization, but the dimethylamino groups present in the loops are losing their charge at this pH and
369 lead to an increase in the contribution of the hydrophobic units in the total DIPEC structure. Aggregation of the
370 interacting chains and non-charged fragments in “defects” lead to the formation of hydrophobic entities within
371 the particles. Schematic structures of DPC and DIPEC particles are shown in Fig. 6.

372 According to the chemical structure of IND we can expect IND-EPO interactions, which will influence the drug
373 release rate (Kindermann et al., 2011, 2012; Quinteros et al., 2011a, 2011b; Gusman et al., 2012).

374 Based on these results, the explanation of drug release from this system can be understood as follows. In acidic
375 medium (pH 1.2 and 5.8), macromolecules of EPO hydrate and the copolymer partially dissolves. The solubility
376 of the EPO/IND complex is also relatively high, but in the presence of S100 the release of the drug will decrease
377 significantly. The remaining amount of ionized EPO and EPO/IND complex after transfer to a medium with higher
378 pH will continuously lose charges on dimethylamino groups of the polycation chains, leading to the formation of
379 insoluble fibers in the structure of the particles. At pH 6.8, most of the carboxyl groups of IND are deprotonated
380 but sequences of S100 are still insoluble. Therefore, the repulsive forces between the negative charges of IND in
381 DIPEC structure result in the continuous drug release.

382 The release rate of IND increases when the DPC and DIPEC are transferred into the final medium. According to
383 the above-mentioned explanation, the increase in the release rate in this case at pH 7.4, could be due to the
384 modification of the structure of DIPEC particles during the penetration of dissolution medium into the system.
385 IND molecules, which cannot compete in the interpolyelectrolyte reaction, cannot find free sequences of
386 charged dimethylamino groups in the insoluble fibers of EPO sequences, which will increase drug release.
387 According to FT-IR results observed for polycomplex matrices based on Eudragit® EPO – Eudragit® S100 (Mustafin
388 et al., 2011) we believe that similar processes are possible in the present DIPEC composed of the same
389 copolymers.

390 In order to prove this, measuring the size and zeta potential of DIPEC particles under conditions, mimicking
391 the release process was performed. During the titration, zeta potential and size of DIPEC clearly changed
392 (Fig. 7). Zeta potential values increased up to pH 3.2 (+27.75 mV) followed by a gradual decrease with
393 increasing pH. On the other hand, the particle size was minimal below pH 4.4 and then it increased up to pH
394 5.4 and 6.8 and decreased again at pH 7.4. In our opinion, the behavior of DIPEC particles in acidic medium
395 (the largest size, zeta potential value +26.45 mV) corresponds to the dissolved DIPEC with minor release of
396 IND from the system.

397 With increasing pH values the zeta potential begins to decrease, due to gradually decreasing the charge
398 density of the positively charged EPO sequences, but the particles became larger indicating swelling and the
399 start of IND release as a consequence of the dissociation of DIPEC structure. Additionally, drug molecules could
400 simply diffuse through less swollen particles.

401 *3.3.2 Indomethacin loaded tablets: release tests*

402 As described in section 2.2.10, two kinds of tablets were produced: the first by compressing lyophilized DPC
403 or DIPEC particles (encapsulated IND tablet) and the latter by compressing physical mixtures with the similar
404 compositions (dispersed IND tablet).

405 Both types of dispersed tablets prepared from the physical mixtures disintegrated rapidly after 15 min. The
406 explanation can be found in the fact that the copolymers are acting individually and no inter-polymer and
407 drug-polymer interactions occurs. Indeed, EPO which is used as a gastric soluble film coating material, was
408 already dissolved after 30 min in acidic medium and S100 is not soluble in this medium; tablets prepared

409 from this copolymer almost immediately disintegrated. Therefore, tested physical mixtures (dispersed IND
410 tablets) are clearly not suitable as oral sustained release systems for IND. Our findings are in the line with to
411 those previously reported by our group (Moustafine et al., 2005, 2013).

412 Fig. 8 shows the release profile obtained from DPC and DIPEC tablets with IND (encapsulated IND tablet): in
413 the gastric environment IND was not released at all instead of its release from the particles at about 5%. In
414 case of DPC tablets, after 7 hours, the pH change from pH=1.2 to pH=7.4 caused gradual release of the drug
415 up to its 50% amount due to the dissolution of the particles and further continuous dissociation of the DPC
416 structures (the complete tablet disintegration was observed within the first 2 hours). So, in this case the
417 release profile of IND is the same as we observed with DPC particles due to the fast disintegration of the
418 tablet (very low stability of the matrices) in acidic environment and similar mechanism of the drug release
419 after the dissociation of the DPC starts. The different release profiles in case of DIPEC systems between
420 tableted (Fig. 8) and powdered particles (Fig. 5) with IND, is obviously due to the reduction of surface area
421 exposed to the dissolution medium: particles, having a greater surface area than the tablets, are more
422 exposed to the dissolution medium and then the release of the drug is more rapid compared to tablets with
423 IND, in which, instead, the fluid must first penetrate the interstices between the particles placed in close
424 contact to each other, which is in accordance with the literature (Dalmoro et al., 2017). Moreover, a visible
425 transparent hydrogel layer is formed around the less swollen matrix DIPEC tablets in acidic medium (in the
426 first hour). However, the front of the external layer appeared turbid at pH=5.8 as the pH rises. This is in
427 agreement with our previous findings, concerning oppositely charged systems made of Eudragit EPO/L100
428 matrices during swelling in GIT mimicking conditions (Moustafine et al., 2013). The reason for it is the
429 influence of gastroresistant S100 copolymer, which plays an important role as additional hydrophobic layer
430 forming component. This makes it less penetrable to drug diffusion from the swollen DIPEC matrix, stable
431 until the end of the experiment. Additionally, the rate of the drug dissociation within swollen matrices is also
432 significantly decreased under these conditions.

433 Based on the results generated, we can conclude that unique properties of the EPO-S100 interpolyelectrolyte
434 complexes, which could be easily regulated by changing their composition and charge density, should be
435 applicable for the design of precisely pH-controlled drug-interpolyelectrolyte ternary systems for colon-targeting
436 of the encapsulated drugs.

437 **4. Conclusions**

438 The results of the present investigation confirm the formation of a novel particulate system composed of
439 interpolyelectrolyte complexes between EPO and S100 in the presence of anionic IND. The formation and
440 chemical composition of ternary systems based on drug-interpolyelectrolyte complex (DIPEC) was established
441 by gravimetry, UV-spectrophotometry, capillary viscosity and elemental analysis and confirms that DIPEC is
442 formed in molar ratio EPO/L100/IND of 4.5:1:1. The particles are spherically shaped with a mean particle size

443 of 500 nm and with a positive zeta potential. Spectroscopic (FTIR, NIR and Raman) and solid state analytical
444 methods (MDSC, XRPD) confirm that IND, included in DIPEC, was in the amorphous state. These particles are
445 able to strongly protect the drug from the gastric environment and could be suitable for colon-targeting
446 purposes. Finally, particles loaded with indomethacin were used to prepare tablets, with a slower IND release,
447 which can potentially be used as oral pH-controlled drug delivery systems for sustained indomethacin release.

448 **Author information**

449 *Corresponding author*

450 *R.I.M.: Kazan State Medical University, Department of Pharmaceutical, Toxicological and Analytical
451 Chemistry; Butlerov str., 49; 420012 Kazan; Tatarstan; Russian Federation; e-mail,
452 rouslan.moustafine@gmail.com; tel, +7(843) 5213782; fax: +7(843) 2360393.

453 **Acknowledgments**

454 This work is, in part, financially supported by the Russian Science Foundation via grant 14-15-01059 (to R.M.,
455 A.S., A.B., S.N and T.K.). The authors acknowledge the Ministry of Education and Science of the Republic of
456 Tatarstan (Russia) for “Algarysh” grant supporting V.V.K. visits to Kazan State Medical University. We are
457 grateful to Dr.Sonja Aškračić at Institute of Physics Belgrade, for her helpful discussion and interpretation of
458 the Raman spectroscopy results. KDSI company (Saint-Petersburg, Russia) is acknowledged for the solid-state
459 particle characterization analysis by using Morphologi G3SE-ID automated system (Malvern Instruments Ltd,
460 Worcestershire, UK).

461 **Notes**

462 The authors declare no competing financial interest.

463 **References**

- 464 Alhnan, M.A., Basit, A.W., 2011. Engineering polymer blend microparticles: an investigation into the influence
465 of polymer blend distribution and interaction. *Eur. J. Pharm. Sci.* 42, 30–6.
- 466 Amidon, S., Brown, J.E., Dave, V.S., 2015. Colon-targeting oral drug delivery systems: Design trends and
467 approaches. *AAPS PharmSciTech.* 16 (4), 731–741.
- 468 Bani-Jaber, A.H., Alkawareek, M.J., Al-Gousous, J.J., Abu Helwa, A.Y., 2011. Floating and sustained-release
469 characteristics of effervescent tablets prepared with a mixed matrix of Eudragit L 100-55 and Eudragit E
470 PO. *Chem. Pharm. Bull.* 59 (2), 155–160.
- 471 Basit A.W., 2005. Advances in colonic drug delivery. *Drugs* 65 (14), 1991–2007.

472 Bigucci, F., Angela, A., Vitali, B., Saladini, B., Cerchiara, T., Gallucci, M.C., Luppi, B., 2015. Vaginal inserts based
473 on chitosan and carboxymethylcellulose complexes for local delivery of chlorhexidine: Preparation,
474 characterization and antimicrobial activity. *Int. J. Pharm.* 478, 456–463.

475 Bourganis, V., Karamanidou, T., Kammona, O., Kiparissides C., 2017. Polyelectrolyte complexes as prospective
476 carriers for the oral delivery of protein therapeutics. *Eur. J. Pharm. Biopharm.* 111, 44–60.

477 Chokshi, R.J., Sandhu, H.K., Iver, R.M., Shan, N.H., Malick, A.W., Zia, H., 2005. Characterization of physico-
478 mechanical properties of indomethacin and polymers to assess their suitability for hot-melt extrusion
479 process as a means to manufacture solid dispersion/solution. *J. Pharm. Sci.* 94 (11), 2463–2474.

480 Chokshi, R.J., Shan, N.H., Sandhu, H.K., Malick, A.W., Zia, H., 2008. Stabilization of low glass transition
481 temperature indomethacin formulations: Impact of polymer-type and its concentration. *J. Pharm. Sci.* 97
482 (6), 2286–2298.

483 Cilurzo, F., Minghetti, P., Casiraghi, A., Montanari, L., 2000. Evaluation of compatibility of methacrylic
484 copolymers by capillary viscosimetry. *J. Appl. Polym. Sci.* 76, 1662–1668.

485 Dalmoro, A., Sitenkov, A.Y., Lamberti, G., Barba A.A., Moustafine, R.I., 2016. Ultrasonic atomization and
486 polyelectrolyte complexation to produce gastroresistant shell-core microparticles. *J. Appl. Polym. Sci.*
487 133, 1–9.

488 Dalmoro, A., Sitenkov, A.Y., Cascone, S., Lamberti, G., Barba A.A., Moustafine, R.I., 2017. Hydrophilic drug
489 encapsulation in shell-core microcarriers by two stage polyelectrolyte complexation method. *Int. J.*
490 *Pharm.* 518, 50–58.

491 De Filippis, P., Boscolo, M., Gibellini, M., Rupena, P., Rubessa, F., Moneghini, M., 1991. The release rate of
492 indomethacin from solid dispersions with Eudragit E. *Drug Dev. Ind. Pharm.* 17 (14), 2017–2028.

493 De Robertis, S., Bonferoni, M.C., Elviri, L., Sandri, G., Caramella, C., Bettini, R., 2015. Advances in oral
494 controlled drug delivery: the role of drug—polymer and interpolymer non-covalent interactions. *Exp.*
495 *Opin. Drug Deliv.* 12 (3), 441–453.

496 Gallardo, D., Skalsky, B., Kleinebudde, P., 2008. Controlled release solid dosage forms using combinations of
497 (meth)acrylate copolymer. *Pharm. Dev. Technol.* 13 (5), 413–423.

498 Gazzaniga, A., Palugan, L., Foppoli, A., Sangalli, M.E., Zema, L., 2006. Timed-controlled oral drug delivery for
499 colon targeting. *Exp. Opin. Drug Deliv.* 3 (5), 583–597.

500 Gusman, M.L., Manzo, R.H., Olivera, M.E., 2012. Eudragit E100 as drug carrier: The remarkable affinity of
501 phosphate ester for dimethylamine. *Mol. Pharm.* 9 (9), 2424–2433.

502 Hartig, M.S., Greene, R.R., Dikov, M.M., Prokop, A., Davidson, J.M., 2007. Multifunctional nanoparticulate
503 polyelectrolyte complexes. *Pharm. Res.* 24 (12), 2353–2369.

504 Hédoux, A., Guinet, Y., Capet, F., Paccou, L., Descamps, M., 2008. Evidence for a high-density amorphous
505 form in indomethacin from Raman scattering investigations. *Phys. Rev. B.* 77, 094205.

506 Heinz, A., Savolainen, M., Rades, T., Strachan, C.J., 2007. Quantifying ternary mixtures of different solid-state
507 forms of indomethacin by Raman and near-infrared spectroscopy. *Eur. J. Pharm. Sci.* 32, 182–192.

508 Hua, S., Marks, E., Schneider, J.J., Keely, S., 2015. Advances in oral nano-delivery for colon targeted drug
509 delivery in inflammatory bowel disease: Selective targeting to diseased versus healthy tissue.
510 *Nanomedicine: Nanotechnology, Biology, and Medicine* 11, 1117–1132.

511 Kabanov V.A., 2005. Polyelectrolyte complexes in solution and in bulk. *Russ. Chem. Bull.* 74 (1), 3–20.

512 Kao, J.Y., McGoverin, C.M., Graeser, K.A., Rades, T., Gordon, K.C., 2012. Measurement of amorphous
513 indomethacin stability with NIR and Raman spectroscopy. *Vibrat. Spectr.* 58, 19–26.

514 Kemenova, V.A., Moustafine, R.I., Alekseyev, K.V., Scorodinskaya, A.M., Zezin, A.B., Tenchova, A.I., Kabanov,
515 V.A., 1991. Applying interpolymer complexes in pharmacy. *Pharmacya* 60 (1), 67–72.

516 Khutoryanskiy, V.V., 2007. Hydrogen-bonded interpolymer complexes as materials for pharmaceutical
517 applications. *Int. J. Pharm.* 334, 15–26.

518 Kindermann, C., Matthee, K., Sievert, F., Breitzkreutz, J., 2012. Electrolyte-stimulated biphasic dissolution
519 profile and stability enhancement for tablets containing drug-polyelectrolyte complexes. *Pharm. Res.* 29
520 (10), 2710–2721.

521 Kindermann, C., Matthee, K., Strohmeyer, J., Sievert, F., Breitzkreutz, J., 2011. Tailor-made release triggering
522 from hot-melt extruded complexes of basic polyelectrolyte and poorly water-soluble drugs. *Eur. J. Pharm.*
523 *Biopharm.* 79, 372–381.

524 Lankalapalli, S., Kolapalli, V.R.M., 2009. Polyelectrolyte complexes: A review of their applicability in drug
525 delivery technology. *Ind. J. Pharm. Sci.* 71, 481–487.

526 Liu, H., Wang, P., Zhang, X.; Shen, F.; Gogos, C.G., 2010. Effects of extrusion parameters on the dissolution
527 behavior of indomethacin in Eudragit® E PO solid dispersions. *Int. J. Pharm.* 383, 161–169.

528 Liu, H., Zhang, X., Suwardie, H., Wang, P., Gogos, C.G., 2012. Miscibility studies of indomethacin and Eudragit®
529 E PO by thermal, rheological, and spectroscopic analysis. *J. Pharm. Sci.* 101 (6), 2204–2212.

530 Lorenzo-Lamoza, M.L., Remuñán-Lopez, C., Vila-Jato, J.L., Alonso, M.J., 1998. Design of microencapsulated
531 chitosan microspheres for colonic drug delivery. *J. Control. Release* 52, 109–118.

532 Maroni, A., Del Curto, M.D., Zema, L., Foppoli, A., Gazzaniga, A., 2013. Film coatings for oral colon delivery.
533 *Int. J. Pharm.* 457, 372–394.

534 Moustafine, R.I., 2014. Role of macromolecular interactions of pharmaceutically acceptable polymers in
535 functioning oral drug delivery systems. *Russ. J. Gen. Chem. J.* 84 (2), 364–367.

536 Moustafine, R.I., Bobyleva, O.L., 2006. Design of new polymer carriers based of Eudragit® EPO/Eudragit® L100-
537 55 interpolyelectrolyte complexes using swellability measurements. *J. Control. Release* 116 (2), e35–
538 e36.

539 Moustafine, R.I., Bobyleva, V.L., Bukhovets, A.V., Garipova, V.R., Kabanova, T.V., Kemenova, V.A., Van den
540 Mooter, G., 2011. Structural transformations during swelling of polycomplex matrices based on

541 countercharged (meth)acrylate copolymers (Eudragit® E PO/Eudragit® L 100-55). *J. Pharm. Sci.* 100 (3),
542 874–885.

543 Moustafine, R.I., Kabanova, T.V., Kemenova, V.A., Van den Mooter, G., 2005. Characteristics of
544 interpolyelectrolyte complexes of Eudragit E100 with Eudragit L100. *J. Control. Release* 103, 191–198.

545 Moustafine, R.I., Zaharov, I.M., Kemenova, V.A., 2006. Physicochemical characterization and drug release
546 properties of Eudragit® E PO/Eudragit® L100-55 interpolyelectrolyte complexes. *Eur. J. Pharm. Biopharm.*
547 63 (1), 26–36.

548 Mustafin, R.I., 2011. Interpolymer combinations of chemically complementary grades of Eudragit
549 copolymers: A new direction in the design of peroral solid dosage forms of drug delivery systems with
550 controlled release (review). *Pharm. Chem. J.* 45 (5), 285–295.

551 Mustafin, R.I., Bobyleva, O.L., Bobyleva, V.L., Van den Mooter, G., Kemenova, V.A., 2010a. Potential carriers
552 for controlled drugs delivery based on interpolyelectrolyte complexes using Eudragit® types EPO and
553 L100-55. I. Synthesis and comparative physicochemical evaluation. *Pharm. Chem. J.* 44 (6), 319–323.

554 Mustafin, R.I., Bobyleva, V.L., Kemenova, V.A., 2010b. Potential carriers for controlled drugs delivery based
555 on Eudragit® EPO/L100-55 interpolyelectrolyte complexes. 2. Comparative evaluation of diffusion
556 transport properties. *Pharm. Chem. J.* 44 (7), 391–395.

557 Mustafin, R.I., Bukhovets, A.V., Sitenkov, A.Yu., Garipova, V.R., Kemenova, V.A., Rombaut, P., Van den
558 Mooter, G., 2011. Synthesis and characterization of a new carrier based on Eudragit® EPO/S100
559 interpolyelectrolyte complex for controlled colon-specific drug delivery. *Pharm. Chem. J.* 45 (9), 568–574.

560 Mustafin, R.I., Kabanova, T.V., 2004. Synthesis and characterization of an interpolyelectrolyte complex based
561 on Eudragit E100 and L100 copolymers. *Pharm. Chem. J.* 38 (11), 625–627.

562 Mustafin, R.I., Kabanova, T.V., 2005. Diffusion transport properties of polymeric complex matrix systems
563 based on Eudragit E100 and L100 copolymers. *Pharm. Chem. J.* 39 (2), 89–93.

564 Nielsen, L.H., Keller, S.S., Gordon, K.C., Boisen, A., Rades, T., 2012. Spatial confinement can lead increased
565 stability of amorphous indomethacin. *Eur. J. Pharm. Biopharm.* 81, 418–425.

566 Obeidat, W.M., Abu Znait, A.H., Sallam, A.A. 2008. Novel combination of anionic and cationic
567 polymethacrylate polymers for sustained release tablet preparation. *Drug Dev. Ind. Pharm.* 34 (6), 650–
568 660.

569 Palena, M.C., Manzo, R.H., Jimenez-Kalruz, A.F., 2012. Self-organized nanoparticles based on drug-
570 interpolyelectrolyte complexes as drug carries. *J. Nanopart. Res.* 14, 867–878.

571 Palena, M.C., García, M.C., Manzo, R.H., Jimenez-Kalruz, A.F. 2015. Self-organized drug-interpolyelectrolyte
572 nanocomplexes loaded with anionic drugs. Characterization and in vitro release evaluation. *J. Drug Del.*
573 *Sci. Tech.* 30A, 45–53.

574 Pergushov, D.V., Müller, A.H.E., Schacher F.H., 2012. Micellar interpolyelectrolyte complexes. *Chem. Soc.*
575 *Rev.* 41, 6888–6901.

576 Philipp, B., Dautzenberg, H., Linow, K.-J., Kötz, J., Dawydoff, W., 1989. Polyelectrolyte complexes – recent
577 developments and open problems. *Prog. Polym. Sci.* 14 (1), 91–172.

578 Pillay, V., Seedat, A., Choonara, Y.E., Du Toit, L.C., Kumar, P., Ndesendo, V.M.K., 2013. A review of polymeric
579 refabrication techniques to modify polymer properties for biomedical and drug delivery applications.
580 *AAPS PharmSciTech.* 14 (2), 692–711.

581 Priemel, P.A., Laitinen, R., Grohganz, H., Rades, T., Strachan, C.J., 2013a. In situ amorphisation with Eudragit®
582 E during dissolution. *Eur. J. Pharm. Biopharm.* 85, 1259–1265.

583 Priemel, P.A., Laitinen, R., Barthold, S., Grohganz, H., Lehto, V-P., Rades, T., Strachan, C.J., 2013b. Inhibition
584 of surface crystallisation of amorphous indomethacin particles in physical drug-polymer mixtures. *Int. J.*
585 *Pharm.* 456, 301–306.

586 Quinteros, D.A., Manzo, R.H., Allemandi, D.A., 2011a. Design of a colonic delivery system based on cationic
587 polymethacrylate (Eudragit E100)-mesalamine complexes. *Drug Del.* 17 (4), 208–213.

588 Quinteros, D.A., Manzo, R.H., Allemandi, D.A., 2011b. Interaction between Eudragit® E100 and anionic drugs:
589 Addition of anionic polyelectrolytes and their influence on drug release performance. *J. Pharm. Sci.* 100
590 (11), 4664–4673.

591 Sarode, A.L., Sandhu, H.K., Shan, N.H., Malick, A.W., Zia, H., 2013a. Hot melt extrusion (HME) for amorphous
592 solid dispersions: Predictive tools for processing and impact of drug-polymer interactions on
593 supersaturation. *Eur. J. Pharm. Sci.* 48, 371–384.

594 Sarode, A.L., Sandhu, H.K., Shan, N.H., Malick, A.W., Zia, H., 2013b. Hot melt extrusion for amorphous solid
595 dispersions: temperature and moisture activated drug-polymer interactions for enhanced stability. *Mol.*
596 *Pharm.* 10 (7), 3665–3675.

597 Sauer, D., McGinity, J.W., 2009. Properties of theophylline tablets dry powder coated with Eudragit® EPO and
598 Eudragit® L 100-55. *Pharm. Dev. Technol.* 16 (6), 632–641.

599 Siepmann, F., Siepmann, J., Walther, M., MacRae, R.J., Bodmeier, R. 2008. Polymer blends for controlled
600 release coatings. *J. Control. Release* 125, 1–15.

601 Sipos, P., Szabó, A., Erös, I., Pirooska Szabó-Révész., 2008. A DSC and Paman spectroscopy study of microspheres
602 prepared with polar cosolvents by different techniques. *J. Therm. Anal. Cal.* 94, 109–118.

603 Tanabe, S., Higashi, K., Umino, M., Limwikanant, W., Yamamoto, K., 2012. Yellow coloration phenomena of
604 incorporated indomethacin into folded sheet mesoporous materials. *Int. J. Pharm.* 429, 38–45.

605 Thünemann, A.F., Müller, M., Dautzenberg, H., Joanny, J-F., Löwen, H., 2004. Polyelectrolyte complexes. *Adv.*
606 *Polym. Sci.* 166, 113–171.

607 Tsuchida, E., 1994. Formation of polyelectrolyte complexes and their structures. *J. Macromol. Sci. Pure Appl.*
608 *Chem.* A31, 1–15.

609 Van den Mooter, G., Colon drug delivery. 2006. *Exp. Opin. Drug Deliv.* 3 (1), 111–125.

610 Wulff, R., Leopold, C.S., 2014. Coatings from blends of Eudragit® RL and L55: a novel approach in pH-
611 controlled drug release. *Int. J. Pharm.* 476, 78–87.

612 Wulff, R., Leopold, C.S., 2016. Coatings of Eudragit® RL and L-55 Blends: Investigations on the drug release
613 mechanism. *AAPS PharmSciTech.* 17 (2), 493–503.

614 List of Tables and Figures

615
616 **Table 1. Composition of DIPEC and physical mixture according to element analysis.**

617 **Table 2. Properties of DIPEC (EPO/S100/IND) particles.**

618 **Table 3. MDSC data of IPEC EPO/S100, DPC (EPO/IND) and DIPEC (EPO/S100/IND).**

619
620
621 **Figure 1. Gravimetric analysis of precipitates and UV-spectrophotometry analysis of supernatant solutions prepared**
622 **at different molar ratios: a) EPO/IND systems, b) EPO/S100/IND systems (n=3; ±SD).**

623 **Figure 2. Relative viscosity of the supernatant solutions of EPO/S100/IND systems as a function of the molar ratio**
624 **(n=3; ±SD).**

625 **Figure 3. ATR-FTIR-spectra of Indomethacin (a), physical mixture (b) DIPEC (c) and PDC (d).**

626 **Figure 4. NIR-spectra of: IND, physical mixture and DIPEC (a); IND, EPO and S100 (b).**

627 **Figure 5. IND release profiles in GIT mimicking conditions of the pure IND and from systems based on DPC EPO/S100**
628 **and DIPEC EPO/S100/IND (n=3; ±SD).**

629 **Figure 6. Schematic representation of DPC (a) and DIPEC (b) structures.**

630 **Figure 7. Zeta potential (blue line) and particle size (red line) of DIPEC dispersions as a function of the pH values during**
631 **automatic titration technique in GIT mimicking conditions (n=3; ±SD).**

632 **Figure 8. IND release profiles in GIT mimicking conditions from tablets based on DPC EPO/S100 and DIPEC**
633 **EPO/S100/IND systems (n=3; ±SD).**

634 635 Supporting information

636 **Figure S1. Particles characterization of DIPEC systems: dimensions (a), morphology (b) and identity (c), according to**
637 **Raman spectra.**

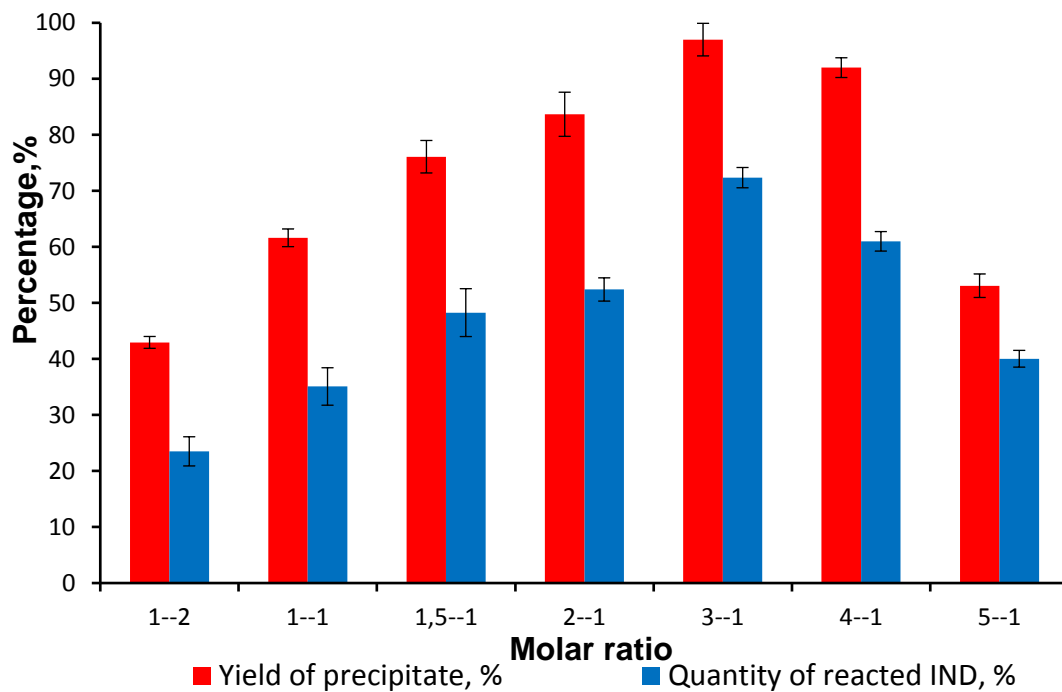
638 **Figure S2. Raman-spectra of: IND, physical mixture and DIPEC (a); EPO, S100 and IPEC (b).**

639

640 **Figure S3: XRPD patterns of the DPC EPO/IND (red line), DIPEC EPO/S100/IND (blue line) and physical mixtures (PM)**
641 **of similar compositions: for EPO/IND (black line), EPO/S100/IND (pink line).**

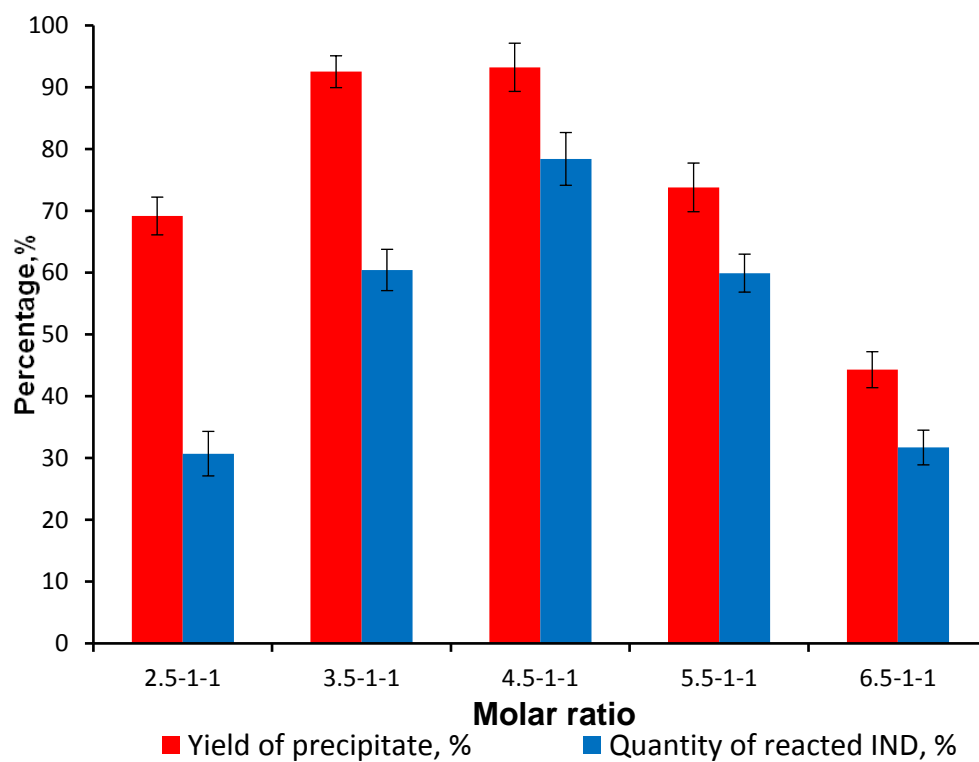
642

644 (a)



645

646 (b)



647

648

649 **Fig. 1.** Gravimetric analysis of precipitates and UV-spectrophotometry analysis of supernatant solutions prepared at
650 different molar ratios: a) EPO/IND systems, b) EPO/S100/IND systems (n=3; \pm SD).
651

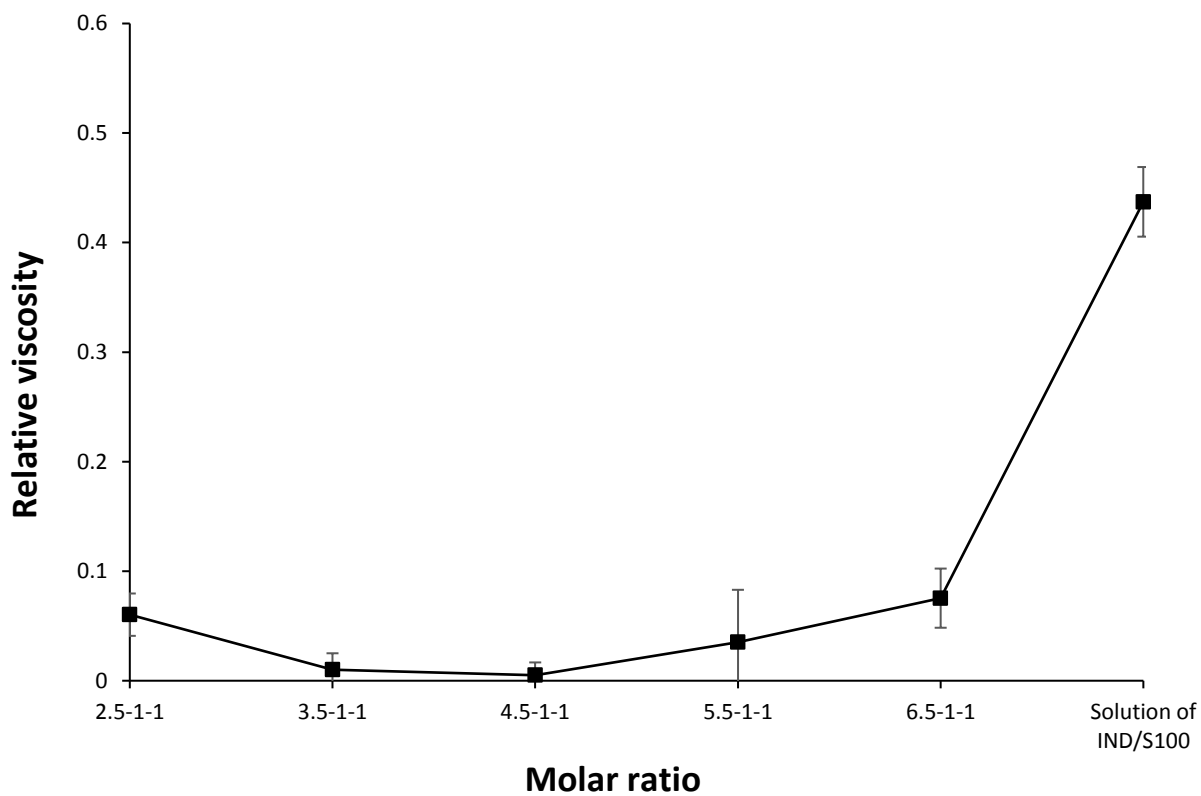
652

653

654

655

656

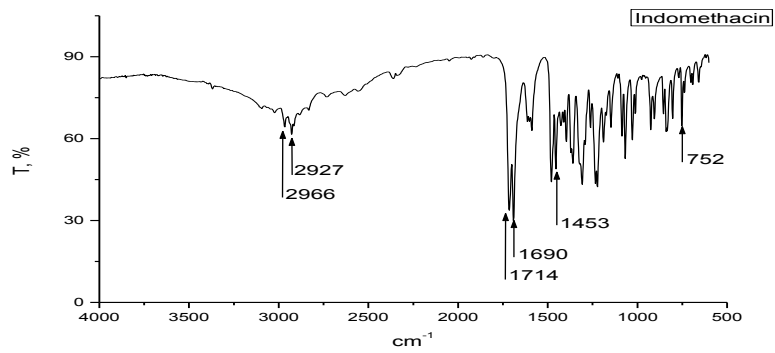


657

658

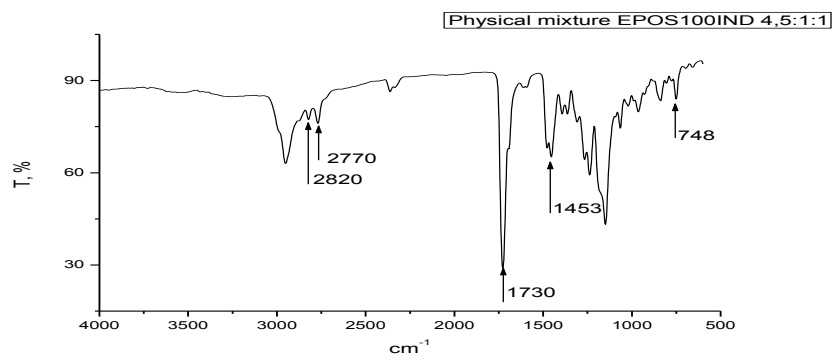
659 **Fig. 2.** Relative viscosity of the supernatant solutions of EPO/S100/IND systems as a function of the molar ratio (n=3;
660 \pm SD).
661

662 a)



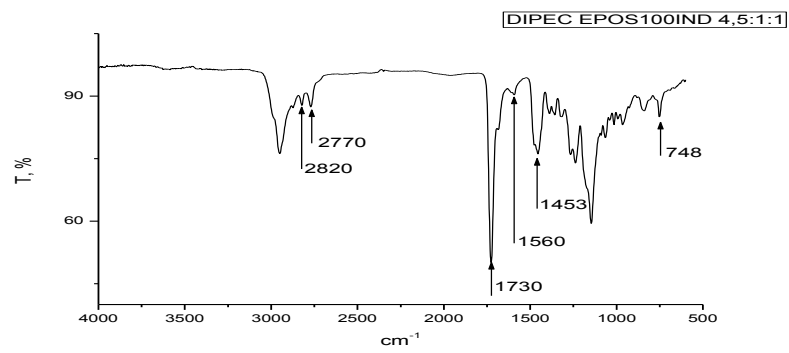
663

664 (b)



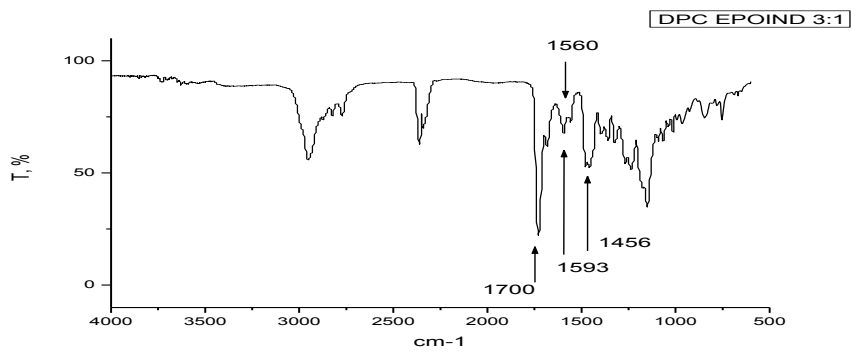
665

666 (c)



667

668 (d)

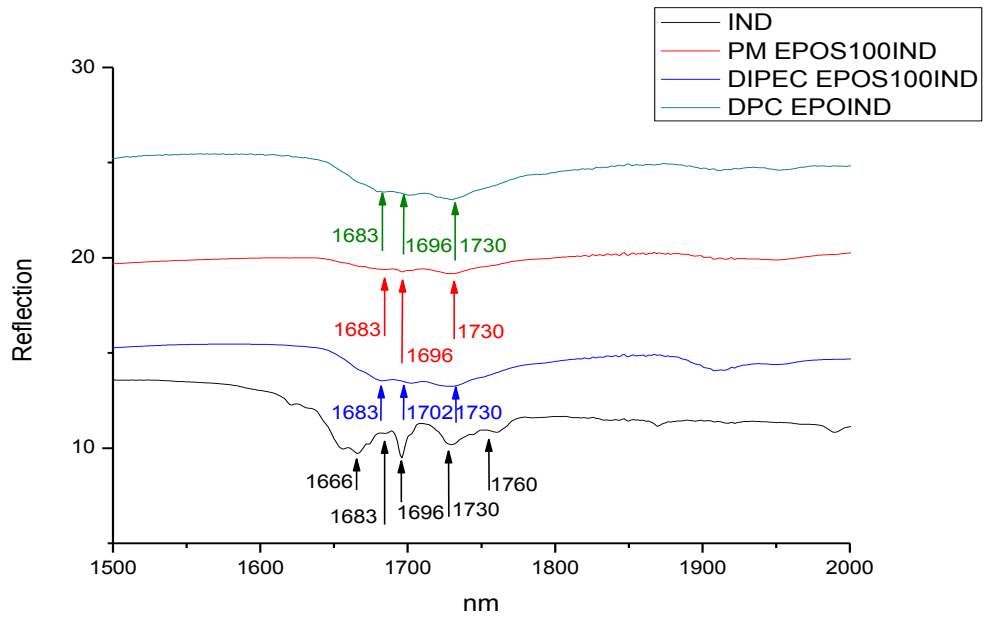


669

670 **Fig. 3.** ATR-FTIR-spectra of Indomethacin (a), physical mixture (b) DIPEC (c) and PDC (d).

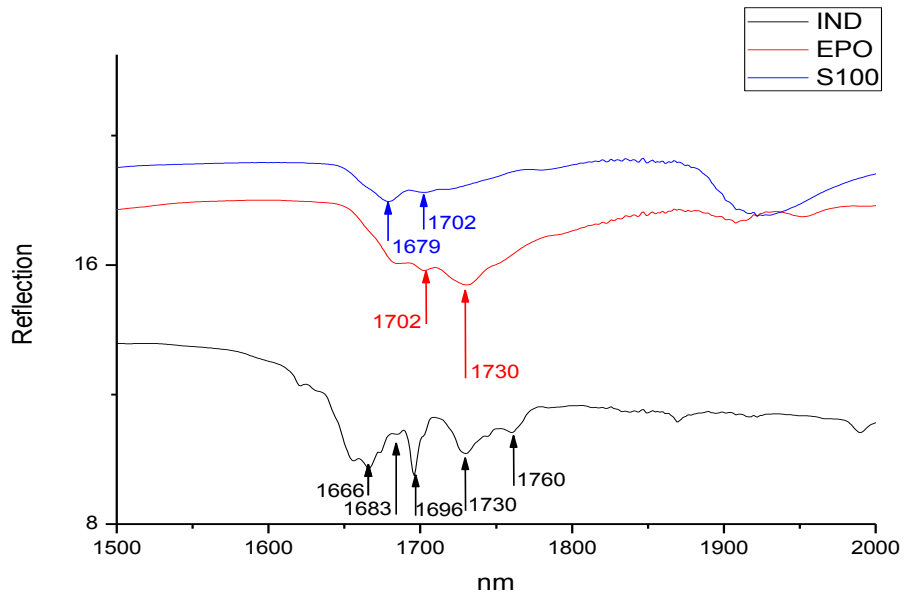
671

672 (a)



673

674 (b)



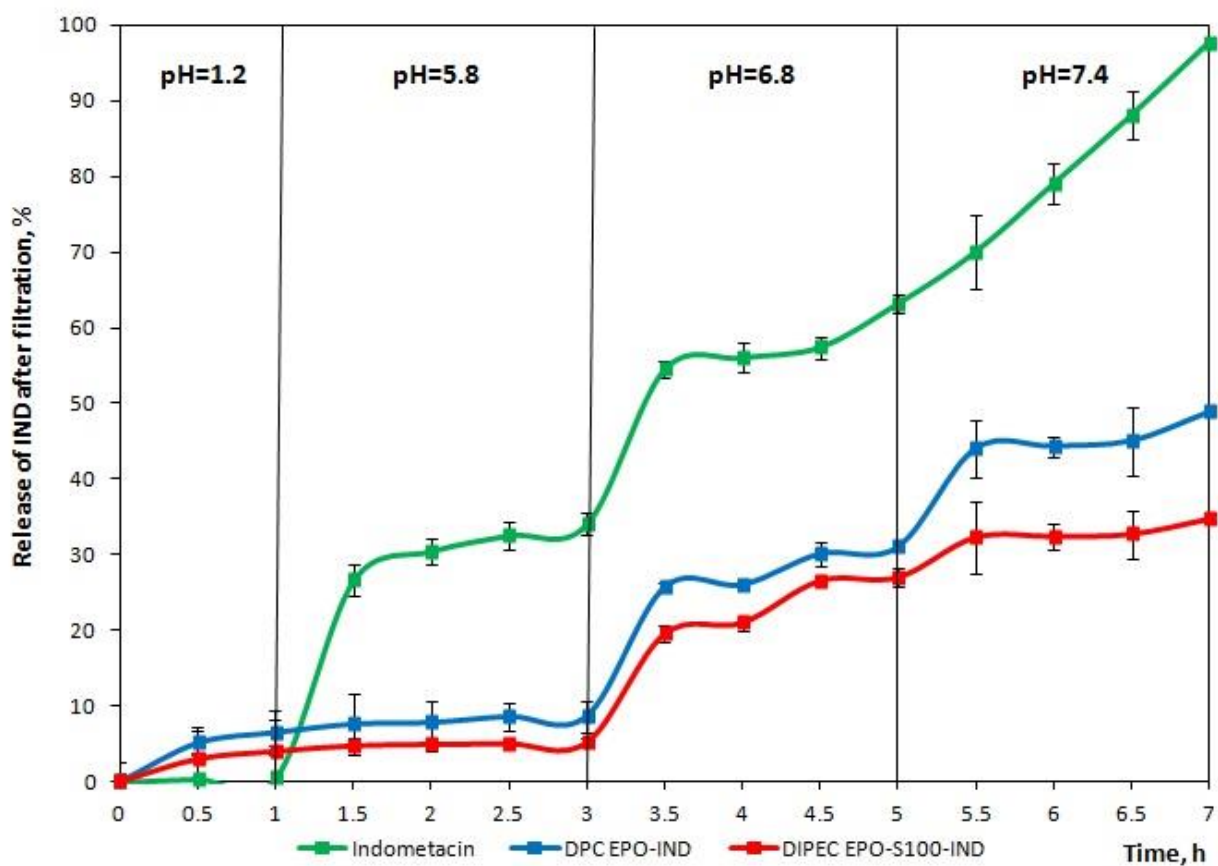
675

676

677

Fig. 4. NIR-spectra of: IND, physical mixture, DIPEC and DPC (a); IND, EPO and S100 (b).

678
679
680
681
682
683
684
685



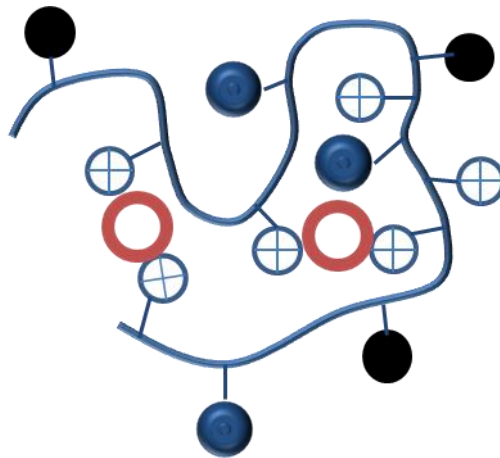
686
687
688
689
690
691
692
693
694
695
696
697

Fig. 5. IND release profiles in GIT mimicking conditions of the pure IND and from particles based on DPC EPO/S100 and DIPEC EPO/S100/IND systems (n=3; \pm SD).

698

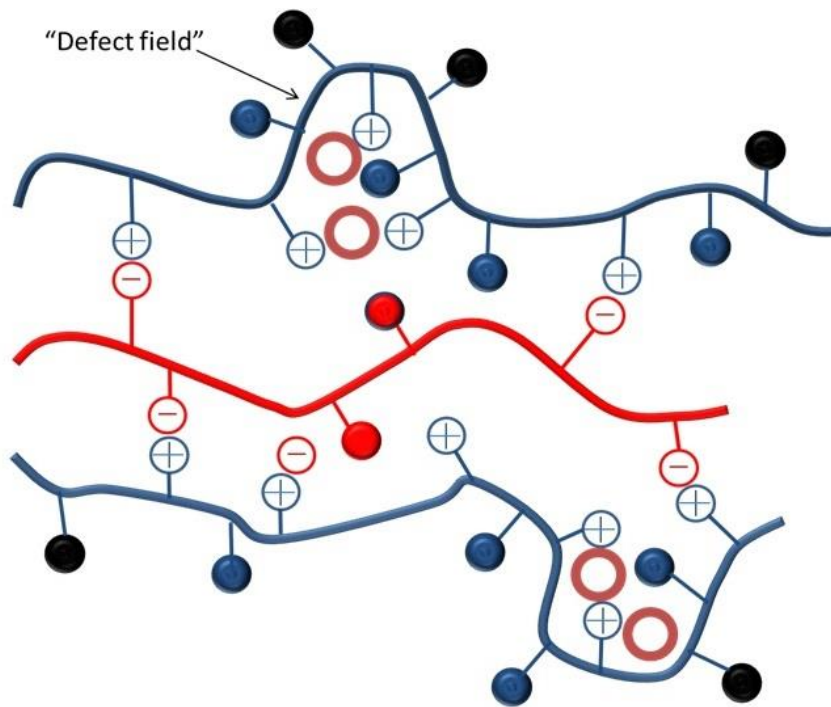
699

700 (a)



701

702 (b)



	$-NH(CH_3)_2$			$-COO^-$
	$-CH_3; -C_4H_9$			$-C_2H_5$
	$-N(CH_3)_2$			$-COOH$
EPO		IND	S100	

703

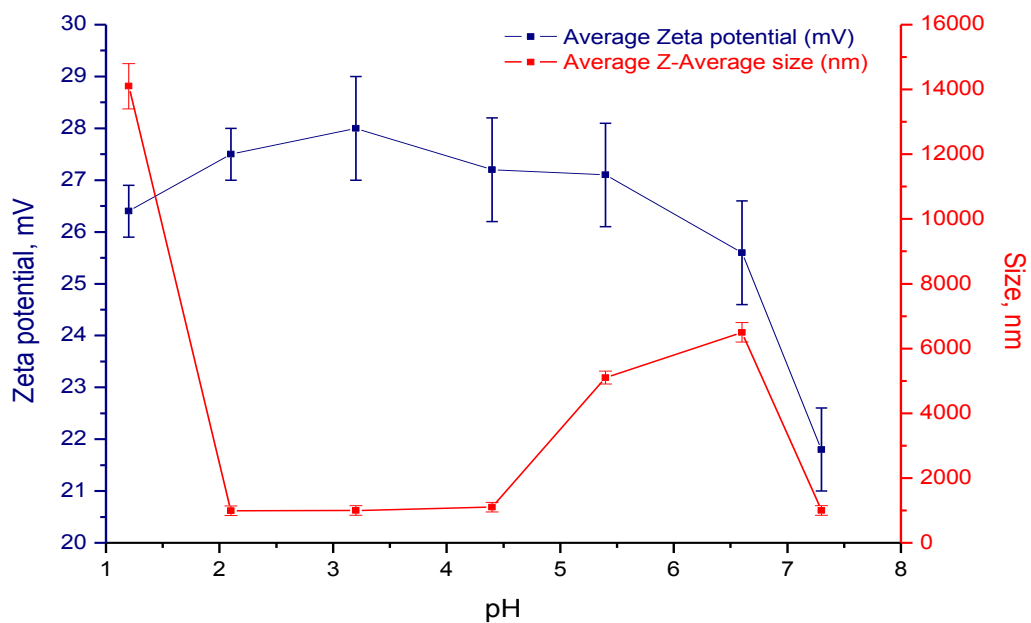
704

705 **Fig. 6.** Schematic representation of DPC (a) and DIPEC (b) structures.

706

707

708



710

711 **Fig. 7.** Zeta potential (blue line) and particle size (red line) of DIPEC dispersions as a function of the pH values during
712 automatic titration technique in GIT mimicking conditions (n=3; \pm SD).
713

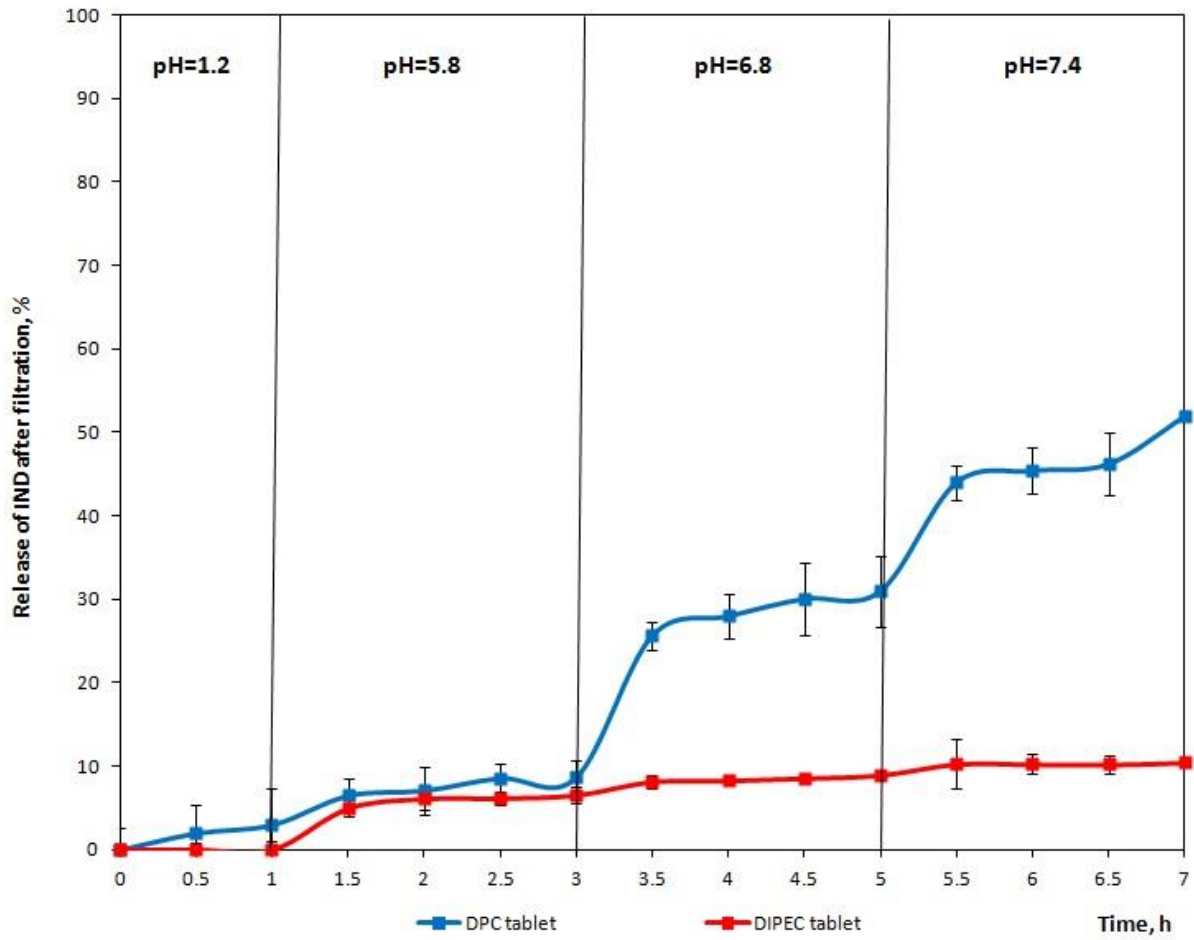
714

715

716

717

718



718

719

Fig. 8. IND release profiles in GIT mimicking conditions from tablets based on DPC EPO/IND and DIPEC EPO/S100/IND systems (n=3; \pm SD).

720

721

722

723

724

725

726

727

728

729

730

731

732

733

734

735